Hindawi
Mobile Information Systems
Volume 2022, Article ID 1116781, 11 pages
https://doi.org/10.1155/2022/1116781

Research Article

Correlation between Vegetation Coverage and Thickness of Chestnut Soil Layer in Typical Grassland Based on Multisource Satellite Remote Sensing

Tang Kesi,[1,2,3] Wulan Tuya,[1] Wu Zifeng,[4] Doljin Dash,[2] and Tsedev Bat-Erdene[2]

[1]*Inner Mongolia Normal University, Hohhot, Inner Monglia 010022, China*
[2]*Mongolian National University of Education, Ulaanbaatar 210648, Mongolia*
[3]*Alxa Branch of Inner Mongolia Autonomous Region Environmental Monitoring Station, Alxa, Inner Monglia 750306, China*
[4]*School of Natural Resources, Faculty of Geographical Science, Beijing Normal University, Beijing 100875, China*

Correspondence should be addressed to Wulan Tuya; mtuya@imnu.edu.cn

Received 7 May 2022; Revised 6 June 2022; Accepted 20 June 2022; Published 30 July 2022

Academic Editor: Jiguo Yu

In order to study the correlation between the vegetation coverage of typical grassland and the thickness of chestnut calcium soil layer, three typical geomorphic types of Wuzhumuqin typical grassland in Inner Mongolia were selected as experimental plots. It uses 3S technology and the methods of landscape ecology and geostatistics to test the image data and field quadrat in the past three years. It closely combines vegetation ecology with soil environment, the relationship between soil characteristics and vegetation landscape, and makes a correlation analysis on the synergistic evolution of chestnut soil thickness. The relationship between chestnut soil thickness, soil water content, and vegetation coverage under three different geomorphic conditions was obtained. Based on the quantitative analysis of the temporal and spatial differences between the vegetation coverage of typical grassland and the thickness of chestnut soil, the spatial distribution patterns of different soil types are revealed. Based on Landsat 8 TM image data, this paper makes statistics of vegetation index (NDVI) at three test sites. The spatial overlap method and the actual observation data are abandoned for spatial interpolation, and the similarity conclusion is obtained. The study shows that among the three sample plots in 2021, except for the original wavy high flat sample plot whose natural environment has been greatly damaged, the correlation coefficient between chestnut calcium soil layer thickness and vegetation coverage in the other two sample plots is also significant in the significance of 0.01 or 0.05 (two-sided test). It shows that there is a very significant positive correlation between the thickness of chestnut calcium soil layer and the thickness of chestnut calcium soil layer. The purpose of this paper is to use hyperspectral images to classify different kinds of plants, so as to realize the monitoring of chestnut soil. It will provide rapid and dynamic technical support for desertification control in the future.

1. Introduction

Typical grassland chestnut soil, about 10–40 cm thick, is similar to human skin. Under the chestnut soil, there is a layer of soft sand. If overgrazing or man-made destruction occurs, then once the vegetation is destroyed, desertification will occur. Due to the increase of surface exposure rate, it creates good ecological conditions for soil and water loss, and wind erosion intensifies the desertification of grassland, thus forming a vicious circle. The change of ecological environment and the interaction of wind erosion promote the degradation and desertification of grassland. Soil is the basic component of the surface system, while the typical meadow vegetation and chestnut soil have formed a certain structure, spatial heterogeneity, and spatial distribution pattern through a long historical process and the comprehensive action of nature and man. The spatial heterogeneity of grassland soil is closely related to typical grassland plants. Due to the lack of sufficient understanding of the spatial heterogeneity of grassland vegetation and soil in China, some sand source control projects often have blind planning in the implementation process, which has not received due

attention. For example, the "enclosure" project is highly arbitrary and cannot be applied to specific needs. China has done a lot of work in grassland ecosystem evolution and grazing intensity, and has monitored grassland degradation by using the advantages of fast, dynamic, and large-scale remote sensing technology. Therefore, the cooperative evolution of grassland vegetation and soil spatial structure was deeply discussed. Through the application of 3S technology, the relationship between vegetation and soil is closely related, and multi-dimensional correlation analysis is carried out. Hyperspectral images were used to analyze the spectral information of representative plants in order to monitor chestnut soil. It carries out large-scale, rapid, and dynamic monitoring for the construction of typical spatial pattern of grassland vegetation and soil.

Many scholars have provided a lot of references on the academic achievements of the coordinated evolution of vegetation coverage and chestnut calcium soil layer thickness in typical grassland. Miao et al. used data from 634 sites to study the relationship between community habitat (plant functional group (PFG), plant litter (VT), and soil type (st)) and grasshopper occurrence in agricultural and pastoral areas of Inner Mongolia [1]. Meng et al. combined with mobile wind tunnel experiment and wind erosion model, explored the effects of a different vegetation coverage, soil humidity, and wind speed on wind erosion at different positions of slopes in the closed desert grassland of Xilamuren grassland [2]. Zhao et al. took the southern edge of Mu Us sandy land as the study area and used the vector autoregressive (VaR) model method to explore the interaction between sandy land, water consumption, and normalized vegetation index (NDVI) from 2000 to 2018 [3]. Yang et al. studied the plant coverage, plant height, species richness, soil water holding capacity, soil organic carbon (SOC), and total nitrogen (n) on the northern slope of Qilian Mountain at an altitude of 2124 ~ 3665 meters [4]. Li et al. studied the effects of different kinds and quality of litter cover on surface runoff parameters through artificial rainfall simulation test with bare slope as the control [5]. Li et al. discussed the paleoenvironment and its control over the formation of organic rich shale [6]. Lema et al. introduced the concept of co-evolution of global value chain and innovation system, and outlined a framework for studying the interaction between them from the dynamic perspective of multiple trajectories [7]. Ma et al. explored the synergy between social ecological innovation in the sharing economy and the sustainable development of urban system [8]. The academic achievements of these correlation studies are lack of data verification, and multisource satellite remote-sensing technology has certain advantages in data acquisition of correlation studies. Therefore, the relevant studies of multisource satellite remote sensing are summarized next.

Many scholars have provided a lot of references for the research of multisource satellite remote sensing. Zhao et al. proposed the retrieval of farmland surface soil moisture using multisource remote-sensing data and GA-BP neural network for feature dimensionality reduction [9]. Amani et al. studied the spectral separability of five wetland categories in Newfoundland and Labrador (NL), Canada, using field data and multisource optical remote sensing (RS) [10]. Susiluoto et al. designed and implemented a computationally efficient multiscale Gaussian process (GP) software package satGP for remote sensing applications [11]. Ghazouani et al. proposed a strategy for semantic remote sensing image scene interpretation [12]. The data of these studies are not comprehensive, and the results of the research need to be discussed, so they cannot be recognized by the public, popularized, and applied. Therefore, combined with multisource satellite remote sensing and the co-evolution of typical grassland vegetation coverage and chestnut calcium soil layer thickness, this paper studies the correlation between the co-evolution of typical grassland vegetation coverage and chestnut calcium soil layer thickness based on multisource satellite remote sensing. It provides effective data and conclusions.

This paper analyzes the correlation between chestnut soil thickness, vegetation coverage, and soil water content in three different geomorphic test areas from 2020 to 2021. The results showed that the correlation between soil water content and chestnut calcium soil layer thickness was the highest, and there was also a certain correlation between vegetation coverage and soil factors. The innovations of this paper are as follows: (1) starting from the internal relationship and interaction of vegetation soil grassland, this paper uses the methods of landscape ecology and geostatistics. Using continuous ecological variables, the correlation between typical grassland vegetation and chestnut calcium soil layer is given, and the relationship curves between vegetation coverage, chestnut calcium soil layer thickness, and soil water content in two gradient directions in three sample plots are drawn. It lays a solid foundation for further studying the spatial autocorrelation between chestnut calcium soil layer and vegetation coverage. (2) In this paper, the spatial structure of chestnut soil with a different soil coverage and soil thickness is analyzed by using the method of semi-variance function. The spatial distribution of a different soil coverage and chestnut soil thickness was obtained by interpolation through ArcGIS platform, and the correlation analysis was carried out. In this paper, the vegetation coverage of three different terrain test plots is analyzed by using the standard vegetation index (NDVI) method, and compared with the corresponding sample plot test data, a similar proportion is obtained. (3) This paper studied the relationship between chestnut calcareous soil coverage and its coverage under different climatic conditions and different soil types. Below 10 cm of chestnut calcareous soil layer, soil is the main factor for the growth and species evolution of typical grassland plants. Based on the experimental data of three years, this paper establishes the relationship between vegetation coverage represented by chestnut soil and the thickness of chestnut calcareous soil layer. It aims to identify plant types through remote sensing images and monitor the thickness of chestnut calcareous soil layer, so as to establish a large-scale and rapid dynamic monitoring system of representative grassland vegetation and soil spatial pattern, and provide technical reference for desertification control in the future.

2. Correlation between Vegetation Coverage and Chestnut Calcium Soil Layer Thickness in Typical Grassland

Landscape ecology takes the whole landscape as the research object and applies the basic theories and methods of ecology to study the landscape structure and function, landscape dynamic change and interaction mechanism, beautification pattern, optimization of structure, rational utilization, and preservation. Landscape ecology is an interdisciplinary subject with ecology and geography as the main content [13, 14]. The basic theory of landscape ecology is based on ecology, geography, natural hierarchical order, and hierarchical theory in open system [15]. The causality feedback coupling relationship in the system is not only a system theory and cybernetics, but also a problem related to information theory. Landscape ecology takes large time and space as the research object, and the spatial form and ecological process of ecosystem as the research object.

Landscape heterogeneity refers to the changes of different types, combinations, and attributes in space and time. It is an important concept in landscape ecology. The heterogeneity of landscape is mainly reflected in the heterogeneity of time and space, that is, the coupling and heterogeneity of time and space. Spatial heterogeneity is manifested in the diversity of various landscape information at a specific spatial level, but also in different temporal and spatial scales. The heterogeneity of time and space determines the structure, function, nature, and location of landscape system. Therefore, landscape heterogeneity is not only an important part of landscape ecology, but also the theoretical basis and core of this discipline. On the whole, the research on landscape heterogeneity shows three trends: ① spatial heterogeneity, that is, complex spatial layout; ② the heterogeneity of time is mainly manifested in the difference of time; and ③ functional heterogeneity.

Geoscience statistics is based on regional variables and uses variogram to analyze natural phenomena, that is, random, structural, spatial correlation, and dependence. The biggest difference between traditional statistical methods and traditional statistics is that it is not only related to the size of sampling values, but also affected by geographical location and distance, which makes up for the spatial shortcomings of traditional statistics. The theoretical basis of geostatistical analysis includes premise hypothesis, regionalization variable, variation analysis, spatial value evaluation, and so on.

(1) Randomness: geological statistics show that the sample values in the study area are random processes, there is no interdependence between the sample values, and there is some internal regularity.

(2) Normal distribution: the research data shall meet the normal distribution. If it does not meet this assumption, the data shall be converted to meet the normal distribution.

(3) Stationarity: stationarity is divided into quadratic stationarity and implicit stationarity. Quadratic stability assumes that the covariance of any two points is the same at the same distance and direction, and the covariance is only related to its position. In other words, it must meet the following two conditions: first, the local variables in the study area are constants. Second, the covariance of regional variables exists and is consistent; that is, it is not affected by the position of variables, but only depends on the distance between variables.

$$\begin{cases} \Phi[\Delta(\Omega)] = \omega, \\ \Phi[\Delta(\Omega)\omega][\Delta(\Omega + g) - \omega]\Gamma(g). \end{cases} \tag{1}$$

$\Delta(\Omega)$ is the regional variation variable, g is the distance between variables, and ω is the constant.

$$\Delta(\Omega) - \Delta(\Omega + g) = 0. \tag{2}$$

Namely,

$$\zeta[\Delta(\Omega) - \Delta(\Omega + g)] = \Phi[\Delta(\Omega) - \Delta(\Omega + g)]^2. \tag{3}$$

$\Delta(\Omega)$ is said to satisfy the intrinsic hypothesis. Intrinsic hypothesis means that the variance (i.e., variogram) of any two points with the same distance and direction is the same. Intrinsic stationarity is a basic assumption made to obtain the basic repetition law. The uncertainty of prediction results can be predicted and estimated through covariance function and variation function.

Semivariogram:

$$\upsilon(\Omega, g) = \frac{1}{2}\zeta[\Delta(\Omega) - \Delta(\Omega + g)]. \tag{4}$$

Namely,

$$\begin{aligned} \upsilon(\Omega, g) = {} & \frac{1}{2}\Phi[\Delta(\Omega) - \Delta(\Omega + g)]^2 \\ & - \frac{1}{2}\{\Phi[\Delta(\Omega)] - \Phi[\Delta(\Omega + g)]\}^2, \\ & \Phi[\Delta(\Omega + g)]\Phi[\Delta(\Omega)]. \end{aligned} \tag{5}$$

Therefore, the semivariogram can be rewritten as

$$\begin{aligned} \upsilon(\Omega, g) &= \frac{1}{2}\Phi[\Delta(\Omega) - \Delta(\Omega + g)]^2, \\ \upsilon(g) &\frac{1}{2}\Phi[\Delta(\Omega) - \Delta(\Omega + g)]^2. \end{aligned} \tag{6}$$

Specifically expressed as

$$\upsilon(g) = \frac{1}{2\psi(g)}\sum_{\mu=1}^{\psi(g)}\left[\Delta\left(\Omega_\mu\right) - \Delta\left(\Omega_\mu + g\right)\right]^2. \tag{7}$$

The theoretical model of variogram is to simulate the experimental variogram based on the measured data of samples with an appropriate smooth curve and select a specific function to describe it, so as to reflect the spatial variation characteristics and trend of regionalized variables.

(1) Spherical model

$$\tau(g) = \begin{cases} 0, & g = 0, \\ \Theta_0 + \Theta\left(\frac{3}{2}\bullet\frac{g}{\Lambda} - \frac{1}{2}\bullet\frac{g^3}{\Lambda^3}\right), & 0 < g \le \Lambda, \\ \Theta_0 + \Theta, & g > \Lambda. \end{cases} \tag{8}$$

Θ_0 is the nugget constant, $\Theta_0 + \Theta$ is the abutment value, Θ is the arch height, and Λ is the range.

(2) Exponential model

$$\tau(g) = \Theta_0 + \Theta\left(1 - e^{-g/\Lambda}\right). \tag{9}$$

(3) Gaussian model

$$\tau(g) = \Theta_0 + \Theta\left(1 - e^{-g^2/\Lambda^2}\right). \tag{10}$$

(4) Power function model

$$\tau(g) = \varsigma g^{\sigma} (0 < \sigma < 2). \tag{11}$$

(5) Logarithmic function model

$$\tau(g) = \varsigma \log(g). \tag{12}$$

(6) Pure nugget model

$$\tau(g) = \begin{cases} 0, & g = 0, \\ \Theta, & g > 0. \end{cases} \tag{13}$$

The complete spatial valuation process includes ① obtaining original data and data processing and analysis; ② selecting the appropriate model for prediction; and ③ model test.

Kriging interpolation, also known as spatial local interpolation, is a method of unbiased optimal estimation of regionalized variables in a limited area based on variogram theory and structural analysis. It is one of the main contents of geostatistics. Expression of Kriging interpolation,

$$\Xi(\kappa) = \rho(\kappa) + \lambda(\kappa). \tag{14}$$

κ is the point at different positions, which can be considered as the spatial coordinate expressed by longitude and latitude; $\Xi(\kappa)$ is the variable value at κ, which can be decomposed into determined trend value $\rho(\kappa)$ and autocorrelation random error $\lambda(\kappa)$. By changing this formula, different types of Kriging methods can be generated.

The calculation formula of Spearman grade correlation coefficient is

$$\tau_{\kappa} = 1 - \frac{6\sum\theta^2}{\xi - \left(\xi^2 - 1\right)}. \tag{15}$$

θ is the rank difference of each pair of observed values after taking the rank of X and Y, respectively, and ξ is the number of all observed pairs.

Mathematical model of multiple linear regression is

$$\begin{aligned} \Psi &= \eta_0 + \eta_1\Omega_1 + \ldots + \eta_r\Omega_r + \gamma, \\ \Psi_{\mu} &= \overset{\Lambda}{\Psi}_{\mu} + \gamma_{\mu} = \varepsilon_0 + \varepsilon_1\Omega_{\mu 1} + \ldots + \eta_r\Omega_{\mu r} + \gamma_{\mu}. \end{aligned} \tag{16}$$

Ψ is the random observation value, ε_0 is the constant term, γ_{μ} is the residual, and r is the number of independent variables.

Establishing test assumptions to ensure the test level δ,

$$G_0 = \eta_1 = \eta_2 = \ldots = \eta_r = 0. \tag{17}$$

The partial regression coefficients of each population are unequal or not completely equal, with $\delta = 0.05$.

The framework of this paper is shown in Figure 1.

Vegetation coverage reflects the suitability of landscape environmental factors, which is the result of the joint action of natural environment and human factors. Soil thickness is closely related to soil fertility. It is not only a supplementary source of nutrients, but also a repository of mineral elements. At the same time, it is also an important symbol to judge soil erosion and has an important impact on the nutritional status of soil. Due to wind erosion, weathering, and other reasons, soil thickness decreases, and there are nutrient loss and even desertification. Generally, artificial fertilization and other methods can be used to make up for and restore the loss of soil, but the loss of cultivated land yield caused by the reduction of soil layer thickness is difficult to make up. In natural vegetation, the influence of soil thickness on vegetation coverage and surface biomass cannot be ignored. Like other factors, soil thickness and vegetation coverage also have certain spatial heterogeneity; that is, there are certain differences in soil thickness and vegetation coverage in different spatial locations. The process of plant heterogeneity will lead to the heterogeneity of various main components in soil. At the same time, it will also have a reaction on plants and restrict each other. Although the characteristics of different types of soil are not completely consistent with the morphology of plants, they show obvious heterogeneity.

In this paper, spatial interpolation technology is used to transform the collected discrete point data into continuous surfaces. As a special measurement type, it is compared with the distribution of other spatial phenomena. It is an important means to obtain the spatial information of natural geographical elements. On the vast typical grassland, due to the imbalance of vegetation coverage and chestnut soil thickness, this paper uses the spatial interpolation method to study the spatial distribution of plant coverage and chestnut soil thickness.

This paper analyzes the thickness and coverage of chestnut soil in three typical areas by using the method of geostatistics. Their spatial structure and heterogeneity are analyzed, and the spatial distribution between them is analyzed. Through the comparison of spatial distribution maps, it can quickly find desertification areas and focus on their protection, so as to slow down the process of desertification.

The typical grassland covers a vast area. The field survey and sampling of grassland data not only wastes a lot of financial and material resources, but also cannot realize real-

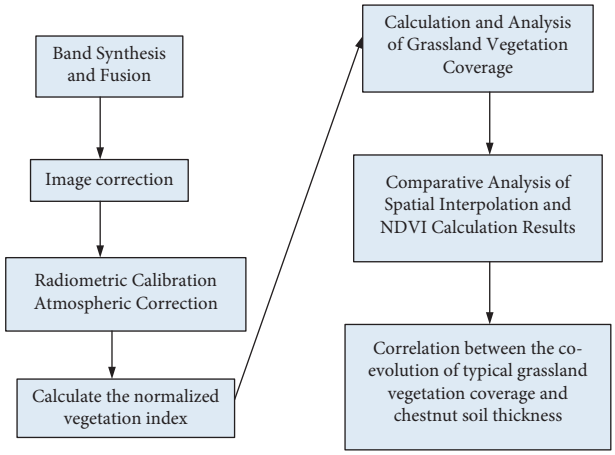

Figure 1: Framework of the article.

time monitoring. Therefore, remote sensing technology, which has many advantages such as fast speed, short cycle, strong timeliness, large area, and higher economic and social benefits, has undoubtedly become the best monitoring method and means. However, in terms of the current development level of remote sensing technology, it is still impossible to directly interpret the thickness of chestnut calcium soil layer in typical grassland with remote sensing images, but the vegetation coverage can be calculated conveniently and quickly with the help of remote sensing images and 3S technology. 3S technology is a general term of remote sensing (RS) technology, geographic information system (GIS), and global positioning system (GPS). It is the combination of space technology, sensor technology, satellite positioning and navigation technology, computer technology, and communication technology. Multidisciplinary highly integrated modern information technology is for the collection, processing, management, analysis, expression, dissemination and application of spatial information. In this paper, Kriging spatial interpolation method is used to compare the spatial distribution of vegetation coverage and chestnut soil thickness of three different terrain test plots, and Landsat 8 TM image data are used to compare the vegetation coverage of three different terrain test plots. In this paper, the spatial superposition analysis method is used to compare this result with the vegetation coverage of three topographic test plots in 2021 based on quadrat test data and Kriging interpolation, so as to judge the similarity between them. It combines the relationship between vegetation coverage and vegetation coverage.

Generally speaking, the preprocessing of remote sensing image includes the following main steps: (1) band synthesis and fusion; (2) image geometric correction; and (3) radiometric calibration and atmospheric correction. Each step is briefly introduced below.

Most of the original data are single band. Landsat satellite data have at least 5 bands and at most 8 bands. Single band data are black and white. At least 3-band synthetic color images are required to meet the research needs. The flowchart of band synthesis is shown in Figure 2. Landsat 8 satellite data have a 15-meter band, and the others are 30 meters. In order to obtain more accurate data, it is

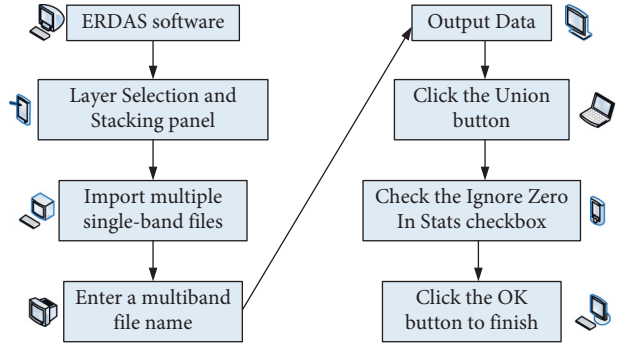

Figure 2: Band synthesis.

necessary to improve the separation rate of the research target image. It needs to fuse the multi-band data synthesized by the front band with the high-resolution band.

The so-called geometric correction is to remove the geometric deformation in the image. The correction methods include systematic, unsystematic, and comprehensive. The main steps of geometric correction are shown in Figure 3.

Radiometric calibration refers to the measurement of physical parameters such as radiance, temperature, and reflectivity. Sensor calibration refers to the method of converting the digital quantization (DN) of the image into physical quantities such as radiance, reflectivity, and surface temperature. Figure 4 shows the step flowchart of radiometric calibration.

The radiation propagation between the sun, ground, and satellite is mainly affected by the scattering and absorption of the atmosphere. Atmospheric correction is very important for the conversion of image gray and ground reflectivity. At the same time, it is very important to match the reflectance of different time and space image data. In order to obtain the true vegetation reflection spectrum, it is necessary to make quantitative atmospheric correction to the remote sensing image. The flowchart of atmospheric correction of satellite remote sensing image is shown in Figure 5.

3. Correlation of Multiparameter Collaborative Evolution

Outliers are individual values in sampling. Its value has significant deviation from other observed values of other samples, and the probability of occurrence is very small. A measurement that exceeds three times the standard deviation is called a high anomaly. During data processing, we should first find out the abnormality, analyze its causes, and then determine whether to exclude it. Due to the existence of specific value, it will have a certain impact on the accuracy of test results, so that the overall characteristics of test data cannot be better reflected. In this paper, the domain method is used to identify outliers, and an average sample is set. Its standard deviation is σ. All data except interval $\overline{X} \pm 3\sigma$ are considered as high outliers, and they are replaced by the maximum and minimum values. In this paper, three types of soil samples from 2020 to 2021 were studied, counted, and analyzed by SPSS software. Then, this paper uses three

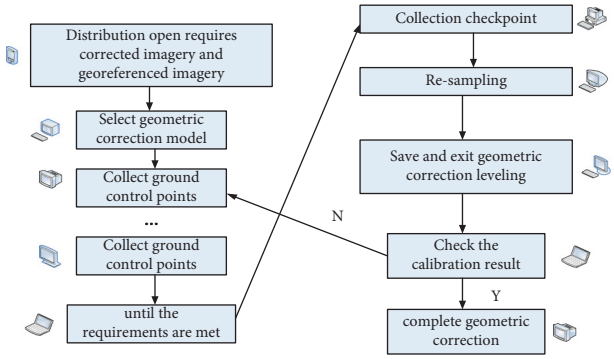

Figure 3: Geometric correction.

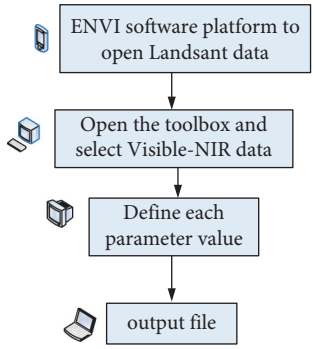

Figure 4: Radiometric calibration.

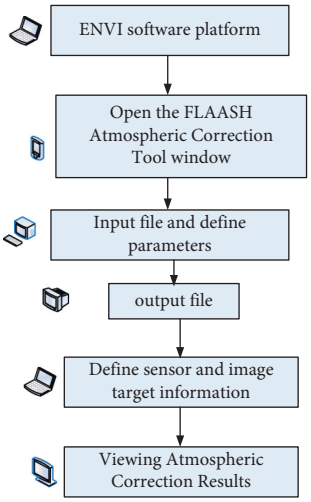

Figure 5: Atmospheric correction.

terrain types as independent variables and the thickness of chestnut soil as variables. The analysis of variance was carried out, and it was compared many times by Tukey HSD and LSD analysis of variance.

In this paper, SPSS software is used to statistically process the test data, and K-S single-point probability method is used to test the normality of three test samples. When p (K-S) > 0.05, the data are normal distribution. The basic statistics of chestnut calcium soil layer thickness in three types of different geomorphic samples from 2020 to 2021 are shown in Tables 1 and 2.

Table 1: Basic statistics of chestnut calcium soil layer thickness in three different geomorphic sample plots in 2020.

Experimental area	Standard error	Mean	Standard deviation
1	0.695	8.653	10.985
2	0.627	7.749	3.458
3	0.794	9.618	8.719

Note. 1—slope landform, 2—low mountain and hilly landform, 3—high plain landform.

Table 2: Basic statistics of chestnut calcium soil layer thickness in three different geomorphic sample plots in 2021.

Experimental area	Standard error	Mean	Standard deviation
1	0.658	7.948	9.918
2	0.318	4.981	4.136
3	0.645	7.369	7.648

It can be seen from Tables 1 and 2 that the thickness of chestnut calcium soil layer of the first two landforms from 2020 to 2021 has passed the normal distribution test of $P = 0.05$ after data transformation, while the high plain landform has not passed the test, but also reached the near-normal distribution. Since the analysis of variance is not particularly strict on the requirements of normal distribution of data, it can also be carried out to achieve near-normal distribution, so the experimental data of this study can be analyzed by one-way ANOVA.

The descriptive statistics of various elements of slope landform and vegetation and the thickness of chestnut calcium soil layer in 2020 and 2021 are shown in Tables 3 and 4.

Tables 3 and 4 show that since the thickness of chestnut calcium soil layer, vegetation coverage, and natural average height of vegetation on the slope fail to pass the K-S normal distribution test, the Pearson product moment correlation coefficient cannot be used for bivariate correlation analysis without data transformation.

The descriptive statistics of various elements of low mountain and hilly landform vegetation and chestnut calcium soil layer thickness in 2020 and 2021 are shown in Tables 5 and 6.

Tables 5 and 6 show that in low mountains and hills, because the thickness of chestnut calcium soil layer, vegetation coverage, and natural average height of vegetation fail to pass the K-S normal distribution test, the Pearson product moment correlation coefficient cannot be used for bivariate correlation analysis without data transformation.

Through the analysis of the data in 2020 and 2021, this paper finds that the soil thickness of chestnut soil has a very weak positive correlation with the natural height of vegetation, while the thickness of chestnut soil has a very weak negative correlation. This result is related to the change of vegetation dominant population during the reduction of chestnut soil thickness. The data analysis in 2021 shows that the correlation between vegetation chestnut calcium soil layer thickness and vegetation coverage has undergone subversive changes. The data processing results are also quite different from those of other experimental areas. Through the field survey of the experimental site, it is found that the

Table 3: Descriptive statistics of chestnut calcium soil layer thickness and vegetation elements in slope plots in 2020.

	Mean	Standard deviation	K-S
Chestnut soil layer thickness	10.003	7.894	0.021
The natural average height of vegetation	24.024	10.842	0.418
Vegetation coverage	37.784	12.437	0.042
Vegetation biomass	269.48	120.417	0.187

Table 4: Descriptive statistics of chestnut calcium soil layer thickness and vegetation elements in slope plots in 2021.

	Mean	Standard deviation	K-S
Chestnut soil layer thickness	9.718	7.948	0.000
The natural average height of vegetation	20.754	8.413	0.006
Vegetation coverage	39.421	11.254	0.081
Vegetation biomass	269.581	137.956	0.142

Table 5: Descriptive statistics of chestnut calcium soil layer thickness and vegetation elements in low hill and mausoleum sample in 2020.

	Mean	Standard deviation	K-S
Chestnut soil layer thickness	4.348	8.123	0.000
The natural average height of vegetation	21.154	9.518	0.078
Vegetation coverage	31.156	10.237	1.254
Vegetation biomass	190.658	100.212	0.326

Table 6: Descriptive statistics of chestnut calcium soil layer thickness and vegetation elements in low hill mausoleum sample in 2021.

	Mean	Standard deviation	K-S
Chestnut soil layer thickness	4.132	5.139	0.000
The natural average height of vegetation	20.353	7.891	0.007
Vegetation coverage	40.024	13.152	0.052
Vegetation biomass	179.486	79.492	0.009

construction of the railway close to the herdsmen's residence and the excavation of the adjacent open-pit coal mine in the wavy high plain experimental area in 2021 have had a great impact on the nearby ecological environment. The average height of vegetation decreased, and the vegetation coverage decreased significantly. There was no vegetation in some areas, and herdsmen built cattle sheds in the experimental area. It occupies a large number of grassland, the nearby vegetation is completely destroyed, the vegetation is sparse and low, and the surface is bare, which is consistent with the results reflected by the experimental data.

The descriptive statistics of soil water content in each experimental area in 2020 and 2021 are shown in Figure 6.

Figure 6 shows that the water content of the three types of landforms in 2020 and 2021 passed the K-S normal distribution test, because the thickness data of chestnut calcium soil layer of the three types of landforms in the past two years failed to pass the K-S normal distribution test.

According to the above results, in three different terrain test areas, when there is little artificial interference, the thickness of chestnut soil has a significant correlation with vegetation coverage and soil moisture content. In order to further explore the variation law of chestnut soil coverage and soil moisture with chestnut soil thickness, 100 and 50 test sites were selected in each test area to study the synergistic evolution relationship between chestnut soil thickness, vegetation coverage, soil moisture content, and chestnut soil thickness. Due to the small difference of rainfall and other relevant natural factors between 2020 and 2021, the difference of vegetation coverage between the two years is small, the formation time of chestnut calcium soil layer is long, and the change is small in just two years. Therefore, taking the data of 2020 as an example, this paper draws the relationship between the thickness of chestnut calcium soil layer, soil water content, and vegetation coverage in three different landforms and directions. The thickness of chestnut soil is abnormally high, especially compared with many adjacent calcareous points. The vegetation coverage on all sides is also relatively high, but it is basically consistent with the surrounding vegetation, mainly sandy land, but there are also some representative grasses and Stipa grandis, with the highest coverage of 17% and 25%. This shows that the thickness of chestnut calcareous layer has a certain impact on the number of plants, but it is not a single limiting factor.

Over the past 50 years, the average annual precipitation of Xiwuzhumuqin banner is about 300 mm. The annual precipitation of the experimental area from 2020 to 2021 is shown in Figure 7.

Figure 7 shows that the average annual total precipitation in 2020 is 518.7 mm, which can represent the level of wet year. The average annual total precipitation in 2020 and 2021

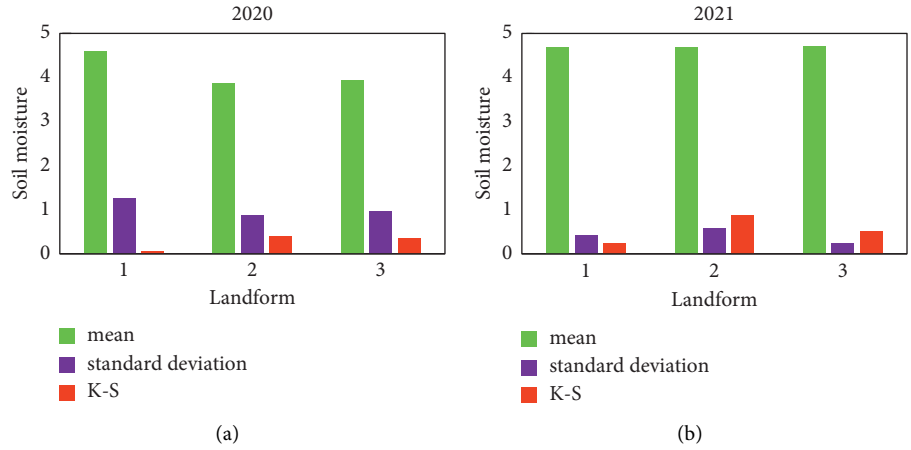

Figure 6: Descriptive statistics of soil water content in each experimental area in 2020 and 2021.

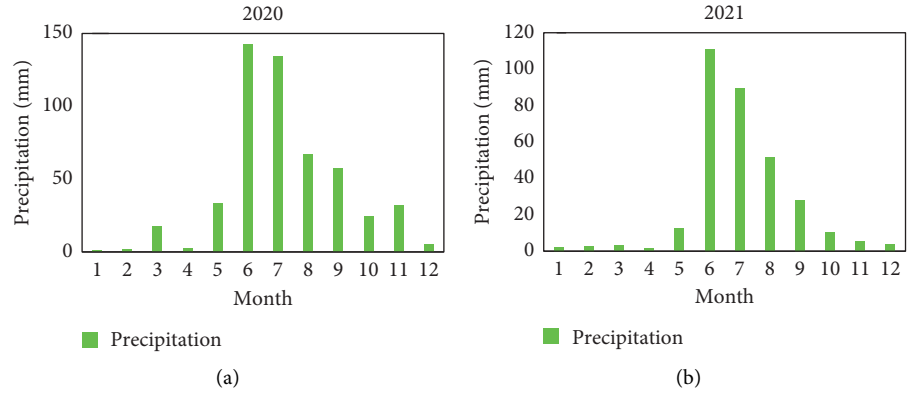

Figure 7: Precipitation from January to December in 2020–2021 experimental area (mm).

is 336.8 mm and 362.6 mm, respectively, which can represent the level of normal year. Because the research interval is short, the interference factors such as natural conditions are close, and the changes of vegetation and soil are not obvious, only the thickness of chestnut calcium soil layer and vegetation coverage data in 2021 is selected for spatial heterogeneity research.

Through the spatial structure analysis of vegetation coverage of three terrain test plots, it is found that the vegetation coverage variation function curves of slope terrain plots and low hill terrain plots are consistent with the spherical model, which is fitted by Gaussian model, as shown in Figure 8.

Nugget value refers to the discontinuous change of regionalized variables when the sample size is less than the sample size. Figure 8 shows the largest nugget value in the slope terrain sample plot. The larger nugget variance shows that some processes on a smaller scale cannot be ignored. In order to improve the spatial structure of data, the method of shortening the sampling interval can be adopted. The base value refers to the half square difference corresponding to the half square difference when the step size increases to a more stable degree. The abutment value of slope terrain sample plot is the highest, 234.00. It shows that the vegetation coverage of slope terrain sample plot has the largest spatial variation, which confirms the largest characteristics of slope terrain sample plot. When the structural ratio is less than 25%, the spatial correlation degree of each variable is relatively low. In the range of 25% ~ 75%, the spatial correlation degree of each variable is medium, while when it is more than 75%, the spatial correlation degree of each variable is very high. Figure 8 shows that the structural proportion of the three test plots is more than 75%, and there is a strong spatial correlation among the test plots; the variation range refers to the distance between sampling points when increasing the variation function from nugget value to base value. The variation range refers to the scope of the spatial dependence of variables, and its variation range is determined by the sampling scale. When the distance between the sampling point and the known point exceeds the range, there is no spatial correlation between the variables. The data values at this point cannot be used for interpolation or extrapolation. The range of change also reflects the spatial continuity of vegetation coverage. In this study, the minimum variation range of the high plain undulating terrain test plot is 100.46 m, while the maximum variation range is 604 m on the low hill terrain. The results show that the continuity order of vegetation cover in the three test plots is

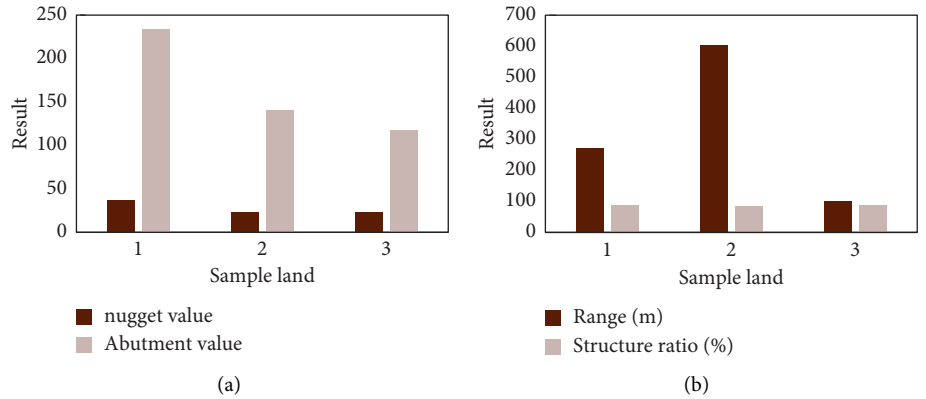

Figure 8: Theoretical fitting model and semi-variance analysis parameters of vegetation coverage in three experimental plots.

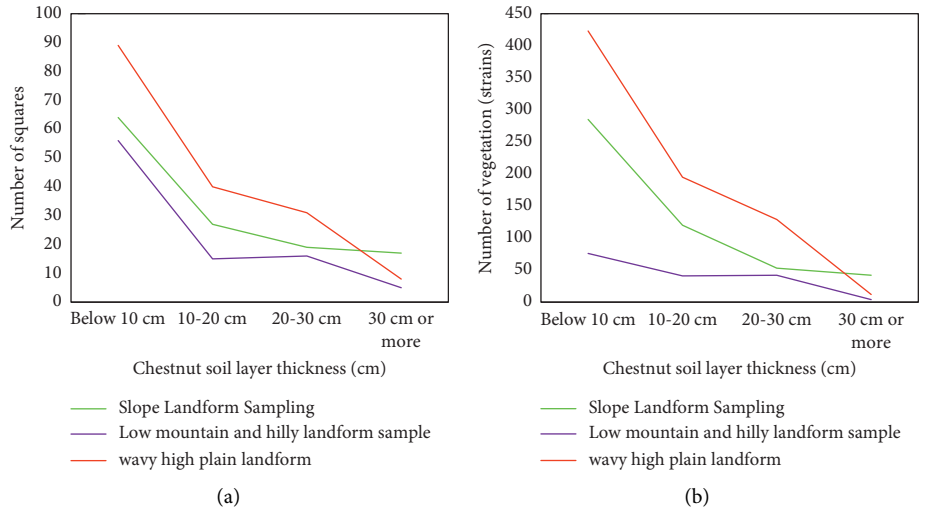

Figure 9: Number of quadrats with cold Artemisia in each grade interval and total density of cold Artemisia in the quadrat.

as follows: the low hill and hill sample plot is significantly higher than the slope plot, and the slope terrain test plot is better than the wavy high plain terrain sample plot.

In order to further study the distribution of Artemisia frigida on the chestnut calcium soil layer with different thicknesses, the quadrats in three different geomorphic sample plots are divided according to the thickness of chestnut calcium soil layer. The thickness of chestnut calcium soil layer is less than 10 cm, the thickness of chestnut calcium soil layer is between 10 ~ 20 cm, the thickness of chestnut calcium soil layer is between 20 ~ 30 cm, and the thickness of chestnut calcium soil layer is more than 30 cm. The purpose is to find the thickness range of chestnut calcium soil layer which is most suitable for the growth of Artemisia frigida. The number of quadrats with cold Artemisia in each grade interval and the total density of cold Artemisia in the quadrat are shown in Figure 9.

Figure 9 shows that Artemisia frigida is a typical grassland plant in different thicknesses of chestnut soil, but when the thickness of chestnut soil is less than 10 cm, the number of Artemisia frigida and Artemisia frigida is significantly higher than other grades. The results showed that the thickness of chestnut calcium soil layer decreased, and its role in the growth and succession of normal grassland became more and more obvious. When the thickness of chestnut calcium soil layer was less than 10 cm. It has an important influence on the growth and evolution of plants, and when the thickness of chestnut soil exceeds 10 cm, it is mainly affected by various factors. The results also show that when the thickness of chestnut soil is less than 10 cm, the protection of chestnut soil should be strengthened to delay the degradation of typical grassland.

In the three sample plots in 2021, except that the ecological damage of wavy Gaoping original sample plot is relatively serious, there is a very significant correlation between chestnut soil thickness and vegetation coverage in the other two sample plots, which are 0.01 ~ 0.05, respectively. Therefore, this paper only discusses the correlation between the coverage and water content of chestnut soil. Due to the difference of soil types, the soil coverage, height, and biomass are high, but the thickness of chestnut soil is low. This is because sand plants such as Salicornia, Artemisia annua, Artemisia frigida, and Caragana microphylla have replaced sand plants. These desert plants are tall, cold, and

drought resistant, so they can grow in the sand even without chestnut soil.

This paper studies the relationship between chestnut soil thickness, soil water content, and vegetation coverage of three different terrain types, and obtains the relationship between soil coverage and chestnut soil thickness and soil water content through field investigation. The results showed that (1) there was a high correlation between soil thickness of chestnut calcium layer and soil moisture. The concurrent layer in some areas can be regarded as linear. With the increase of the thickness of chestnut calcium layer, the wind erosion rate of chestnut calcium layer decreases accordingly. This shows that soil moisture has a significant effect on the thickness of chestnut calcium soil layer. (2) The thickness of chestnut calcium soil layer in some samples is almost zero, but there is still a certain value of soil water content. This is because the soil type of this quadrat is no longer chestnut soil, but completely sandy fine sand, which is fixed by the roots of vegetation and forms hardening when the amount of rain is large. Therefore, although the thickness of chestnut soil layer is zero, the soil water content still has a certain value. (3) The coverage of the thin or even disappeared area of chestnut calcium soil layer is not necessarily small. This is because in the process of wind erosion and desertification of chestnut soil, the population has changed from typical grassland vegetation such as Leymus chinensis and Stipa grandis to sandy plants such as tall Caragana microphylla, Artemisia annua, or low Potentilla stellata. Most of these vegetation have the characteristics of cold and drought resistance. At this time, the typical grassland began to transform into sandy grassland.

In this paper, three typical terrains are studied by using the combination of traditional statistics and geoscience statistics. This paper discusses the coverage degree of different types of soil and the thickness of chestnut soil. On this basis, the following conclusions are drawn: (1) in the three sample plots, the estimation of chestnut soil vegetation coverage and chestnut soil thickness is better than that in the low value area. The calculation results show that the calculation accuracy of this method is in good agreement with the measured values, and the relative error of calculation meets the requirements of this paper. (2) By using Kriging spatial interpolation method, the vegetation coverage of the three sample plots was compared with the thickness of chestnut soil. It is found that the distribution of vegetation coverage and chestnut soil thickness is in good agreement between the slope terrain sample plot and the low hilly mountainous terrain sample plot. On the undulating terrain of the high plain, there is no obvious connection between the spatial distribution of the two. The results showed that under the same interference factors, the response of plant cover to the environment was faster than that of chestnut calcareous soil. Therefore, vegetation coverage is an important index to reflect the characteristics of soil degradation.

Taking Landsat 8 TM satellite data as the research medium, this paper applies the standardized vegetation index on the 3S technology platform after preprocessing such as band synthesis, image correction, radiation correction, and atmospheric correction. It calculates the vegetation coverage of three different terrain test plots in 2021, and compares and analyzes it with the Kriging interpolation results based on the measured quadrat data by using the spatial superposition technology. The results show that they have high consistency in the calculation of vegetation coverage, and it is feasible to use remote sensing technology to monitor vegetation coverage.

4. Conclusion

In this paper, the correlation among soil chestnut thickness, soil water content, and soil water content of three different terrain types was studied by using Spearman rank correlation coefficient. The results showed that except for the wavy height and level in 2021, the chestnut soil thickness, soil water content, and vegetation coverage in other sample plots had significant correlation. The subject of this study is to take Wuzhumuqin typical grassland in Inner Mongolia as an example. The experimental conclusion is not necessarily applicable to all typical grasslands. Therefore, in the subsequent research, it is best to conduct a comprehensive study of China's typical grasslands. The main research results of this paper are as follows: (1) this paper uses multisource remote-sensing data to compare different time phase remote sensing images for change recognition and classification information extraction. (2) Through GPS point sampling, this paper detects the changes of chestnut calcium soil layer thickness and vegetation coverage. Through the interpretation of remote sensing data, this paper calculates the spatial autocorrelation coefficient and tests the significance of autocorrelation. (3) The correlation between indicator species and chestnut calcium soil layer thickness in different succession stages of typical grassland was studied on a small scale, and a mathematical model was established.

Data Availability

The data used to support the findings of this study are available from the corresponding author upon request.

Conflicts of Interest

The authors declare no conflicts of interest.

Acknowledgments

This research study was sponsored by National Natural Science Foundation of China. The name of the project is Comparative study on land desertification in Mongolian Plateau based on country (project no. 41861024).

References

[1] H. T. Miao, Y. Liu, L. Y. Shan, and G. L. Wu, "Linkages of plant-soil interface habitat and grasshopper occurrence of typical grassland ecosystem," *Ecological Indicators*, vol. 90, no. JUL, pp. 324–333, 2018.

[2] Z. Meng, X. Dang, Y. Gao, R. Ding, and M. Wang, "Interactive effects of wind speed, vegetation coverage and soil moisture in controlling wind erosion in a temperate desert steppe, Inner

Mongolia of China," *Journal of Arid Land*, vol. 10, no. 4, pp. 534–547, 2018.

[3] M. Zhao, Y. Wang, S. Liu, Z. Liu, and R. Li, "Correlation assessment of NDVI and land use dynamics with water resources for the southern margin of Mu Us Sandy Land, China," *Environmental Science and Pollution Research*, vol. 29, no. 12, pp. 17049–17061, 2022.

[4] Y. S. Yang, Z. Li, L. Li et al., "Soil physicochemical properties and vegetation structure along an elevation gradient and implications for the response of alpine plant development to climate change on the northern slopes of the Qilian Mountains," *Journal of Mountain Science*, vol. 15, no. 5, pp. 1006–1019, 2018.

[5] Z. Li, B. Wang, and J. Wang, "Effects of Artemisia gmelinii and Bothriochloa ischcemum litter mass coverage on hydrodynamic characteristics of loess overland flow," *Nongye Gongcheng Xuebao/Transactions of the Chinese Society of Agricultural Engineering*, vol. 34, no. 17, pp. 151–157, 2018.

[6] W. Li, S. Lu, Z. Tan, and T. He, "Lacustrine source rock deposition in response to coevolution of the paleoenvironment and formation mechanism of organic-rich shales in the biyang depression, nanxiang basin," *Energy & Fuels*, vol. 31, no. 12, pp. 13519–13527, 2017.

[7] R. Lema, R. Rabellotti, and S. P. Gehl, "Innovation trajectories in developing countries: Co-evolution of global value chains and innovation systems," *European Journal of Development Research*, vol. 30, no. 3, pp. 345–363, 2018.

[8] Y. Ma, K. Rong, D. Mangalagiu, and D. ThorntonZhu, "Co-evolution between urban sustainability and business ecosystem innovation: evidence from the sharing mobility sector in Shanghai," *Journal of Cleaner Production*, vol. 188, no. JUL.1, pp. 942–953, 2018.

[9] J. Zhao, C. Zhang, and L. Min, "Surface soil moisture in farmland using multi-source remote sensing data and feature selection with GA-BP neural network," *Nongye Gongcheng Xuebao/Transactions of the Chinese Society of Agricultural Engineering*, vol. 37, no. 11, pp. 112–120, 2021.

[10] M. Amani, B. Salehi, S. Mahdavi, and B. Brisco, "Spectral analysis of wetlands using multi-source optical satellite imagery," *ISPRS Journal of Photogrammetry and Remote Sensing*, vol. 144, pp. 119–136, 2018.

[11] J. Susiluoto, A. Spantini, H. Haario, T. Härkönen, and Y. Marzouk, "Efficient multi-scale Gaussian process regression for massive remote sensing data with satGP v0.1.2," *Geoscientific Model Development*, vol. 13, no. 7, pp. 3439–3463, 2020.

[12] F. Ghazouani, I. R. Farah, and B. Solaiman, "A multi-level semantic scene interpretation strategy for change interpretation in remote sensing imagery," *IEEE Transactions on Geoscience and Remote Sensing*, vol. 57, no. 11, pp. 8775–8795, 2019.

[13] W. Wen, B. Dou, D. You et al., "Forward a small-timescale BRDF/albedo by multisensor combined BRDF inversion model," *IEEE Transactions on Geoscience and Remote Sensing*, vol. 55, no. 2, pp. 683–697, 2017.

[14] B. A. Johnson, K. Iizuka, M. A. Bragais, and D. B. Magcale-Macandog, "Employing crowdsourced geographic data and multi-temporal/multi-sensor satellite imagery to monitor land cover change: a case study in an urbanizing region of the Philippines," *Computers, Environment and Urban Systems*, vol. 64, no. Jul, pp. 184–193, 2017.

[15] F. Xu, D. Hongtao, C. Zhigang, G. Ming, and M. Shen, "Remote monitoring of cyanobacterial blooms using multi-source satellite data: a case of Yuqiao Reservoir, Tianjin," *Journal of Lake Sciences*, vol. 30, no. 4, pp. 967–978, 2018.